International Journal of Nanoelectronics and Materials
IJNeaM
ISSN 1985-5761 | E-ISSN 2232-1535

Influence of Gamma Radiation on Optical and Morphology Properties for PS and MO/PS Composites

Samah M. Hussein[a], Nahida. J. Hameed[b], Evan T Salim[a,*], Subash C. B. Gopinath[c, d, e]

[a] *Applied Science Department, University of Technology- Iraq, Baghdad, Iraq*
[b] *Al-Farabi University College, Iraq*
[c] *Center for Global Health Research, Saveetha Medical College & Hospital Saveetha Institute of Medical and Technical Sciences (SIMATS), Thandalam, Chennai – 602 105, Tamil Nadu, India*
[d] *Faculty of Chemical Engineering & Technology and Institute of Nano Electronic Engineering, Universiti Malaysia Perlis (UniMAP), 02600 Arau, Perlis, Malaysia*
[e] *Department of Technical Sciences, Western Caspian University, Baku AZ 1075, Azerbaijan*
**Corresponding author. Tel.: +9647715752087; e-mail: evan.t.salim@uotechnology.edu.iq, & evan_tarq@yahoo.com*

ABSTRACT

In this work, the effect of gamma irradiation on optical characteristics of virgin polystyrene (PS) and its composite films was examined. The neat PS and its composites casted to be thin-films both before and after being doped with methyl orange (MO) at weight ratios of 1.0 % wt. /wt. Thickness of the obtained samples varied within the range of 0.2±0.05 mm. The prepared samples were exposed to 1.0, 5.0, and 10 kGy of 60Co (a gamma source) radiation. The optical properties were investigated using ultraviolet-visible spectra within a wavelength range of (280-1100 nm). The samples' absorption spectra were displayed both before and after irradiation. For PS and MO/PS nanocomposites, gamma radiation caused systematic changes in absorption with absorbed doses. The optical bandgap for PS decreased after adding methyl orange dye, and when the gamma ray dose increased from 1.0 to 10 kGy, the direct bandgap decreased from 4.24 to 3.90 eV for PS, and decreased from 4.13 to 3.4 eV for MO/PS. The abovementioned outcome demonstrated by the redshift in the transmittance spectra using Fourier Transform Infrared Spectroscopy (FTIR). The effects of γ-rays on the absorbance, absorption coefficient (α), and extinction coefficient (k) into all the samples were studied, and the findings showed an improvement in parallel with increasing radiation dose. The optical microscope images showed surface damage represented grooves, holes, bubbles, and cracks caused by samples photo-degradation. It was concluded that gamma rays could alter different characteristics of materials in terms of making them suitable for radiation detection, sensing, and dosimetry.

Keywords: *FTIR, Gamma ray, Methyl Orange, Polystyrene, UV-VIS*

1. INTRODUCTION

According to the research work related to polymer science, new elastomers, plastics, adhesives, coatings, and fibers are continuously developed. The new information is gradually consolidated, and standardized with the aid of important new theories about the combination between the technological structures of polymers, their physical properties, and their practical behavior. Thus, the concepts of kinetics, thermodynamics, and polymer chain structure are linked to each other in order to make polymer science stronger. [1, 2]. Ionizing radiation is a green way to create new materials with superior qualities. However, this could change the polymers features because the radiation can break bonds, and create free radicals that might be attached with the reactants to form new entities, giving conventional polymers exceptional properties [3, 4].

The materials and radiation dose have an impact on these properties. Radiation has a significant impact on polymeric materials because it can alter and enhance the physical characteristics of polymers. For instance, when polymeric materials expose to accelerated electrons, X-rays, ion beams, or gamma rays, reactive intermediates are created. These intermediates can subsequently trigger significant reactions like degradation or cross-linking. The specified radiation dose has regulated these interactions [5, 6]. Different polymers respond to radiation doses in different ways, and these responses are intrinsically related to the polymers' chemical structures. Consequently, polymers' optical, electrical, mechanical, and chemical properties are changed [7, 8]. The radiation is limited to ^{60}Co and ^{137}Cs out of thousands of gamma emitters. In addition, gamma rays are electro-magnetic quantum waves with a wavelength that has a shorter and higher photon energy than light [9, 10]. Since gamma rays have become more significant in recent technological advancements, numerous researchers were examined their impact on various polymers comparable to what was previous studies have shown [11-15]. For photonic devices, polymers, particularly poly methyl methacrylate (PMMA) and PS are grown in a popular manner due to their low cost, high flexibility, ease of processing, and customizability [16, 17]. It is known that PS is a substantial component for both industry and academia. PS is a simple chemical compound with a saturated aliphatic chain, and an unsaturated aromatic ring [18-20]. PS is the most preferred polymer for numerous industrial applications due to its exceptional mechanical durability, electrical insulation, low density, strong thermal resistance, ease of molding and processing, and optical transparency

[21-23]. For healthcare sector, PS can play a pivotal role in manufacturing different types of lab apparatus such as Petri dishes and tissue culture, medicinal constituents, trays, containers, medicinal packages, constituents of heart pump, catheters, and epidurals [24-26]. On the other hand, methyl orange is an organic molecule with the molecular formula of (C_{14} H_{14} N_3 Na O_3 S), Methyl Orange is known by its International Nonproprietary Name (INN) as sodium 4-[(4-dimethylaminophenyl) diazenyl] benzenesulfonate. This orange powdery material is a poisonous dye that can be dissolved in water. It can be employed for calibrating a wide range of chemicals [27-29].

The aim of this work is to confirm the impact of gamma irradiation on the optical properties of neat PS and its composite films, which were doped with MO dye. The targeted application related to this work is manufacturing efficient dosimeters. Preparing samples of polymeric systems (pure and composite materials) by dissolution method, then studying of structural, optical properties on them before and after irradiation with γ-ray irradiation at high radiation doses(1,5&10kGy) and studying the change in composition and properties of manufactured specimens.

2. MATERIALS AND INSTRUMENTATION

2. 1 Sample Preparation

For the polymer film, Dichloromethane (CH_2Cl_2) was used to dissolve PS at varying quantities (7–12 wt. /vol), and vigorously stirred using a magnetic stirrer for an hour to create a homogenous solution. The highest concentration needed to produce a film was 10 % wt. /vol. The efficient casting required both bubble-free and easily alighted process from the petri dish. The sample thickness was 0.2±0.05 mm. The SCRC Company supplied methyl orange ($C_{14}H_{14}N_3NaO_3S$), which was added as a dopant to the casted film. To create the MO/PS composites, methyl orange was firstly combined with dichloromethane at a concentration of (1.0 % wt. /wt.), and then dissolved in PS. Figure 1 shows the experimental procedure of casting for preparing the neat polymer and its composites.

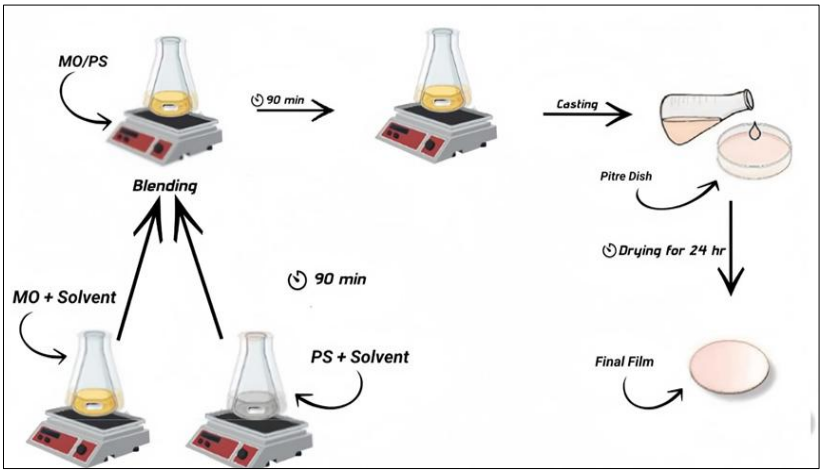

Figure 1. Casting method for preparing the neat polymer and its composites.

2. 2 Instrumentation

To evaluate a precise particle size for Methyl orange, a particle size analyzer (90-plus) was utilized. Figure (2) illustrates the average particle size. The obtained effective diameter for the used nanoparticles was around 12094.1nm (about 12.0941 μm).

The samples were subjected to 14 Gy of gamma-irradiation per hour, with a half-life of 5.3 years, the commonly used Co^{60} Gamma-ray source emits mono-energetic 1.17 and 1.33 MeV γ-rays. Sealed radioactive source Co-60 made in India. And then used_Ultraviolet UV/Visible device. Were carried out using “Shimadzu -1900S” (Japan) in the range of (200-1200nm) to obtain the absorbance value as a function with wavelength. After that, used FTIR Spectroscopy were also conducted using "Shimadzu -1800S" (Japan) within a range of (4000 - 400 cm^{-1}) to determine the molecular structures of both PS as well as the irradiated and non-irradiated MO/PS composites.

The morphology for the prepared samples was analyzed using an Optical Microscope Analysis type MEIJI TECHNO CO.LTD (Japan). Each sample was examined using a magnification power of 100X.

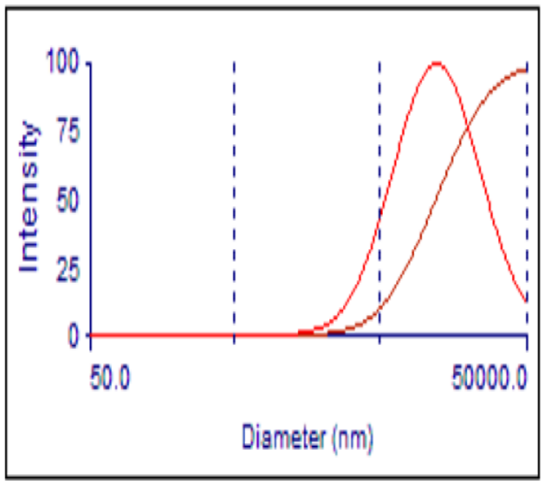

Figure 2. The lognormal size distribution of Methyl Orange.

3. RESULTS AND DISCUSSION

3.1 Effect of Adding MO with PS on Absorption Spectra

The maximum absorbance for MO/PS films was observed at 280 nm, then it rapidly decreased at wavelengths higher than 300 nm, according to Figure (3), which shows the UV-Vis spectra of PS, MO/PS films, and corresponds to unirradiated samples. It is noticed that there was a shift towards longer wavelengths, which can be attributed to the occurrence of localized states within the energy gap. As a result, an increase in absorbance for MO/PS films was achieved. This outcome is in line to what was previously disseminated in [30-32].

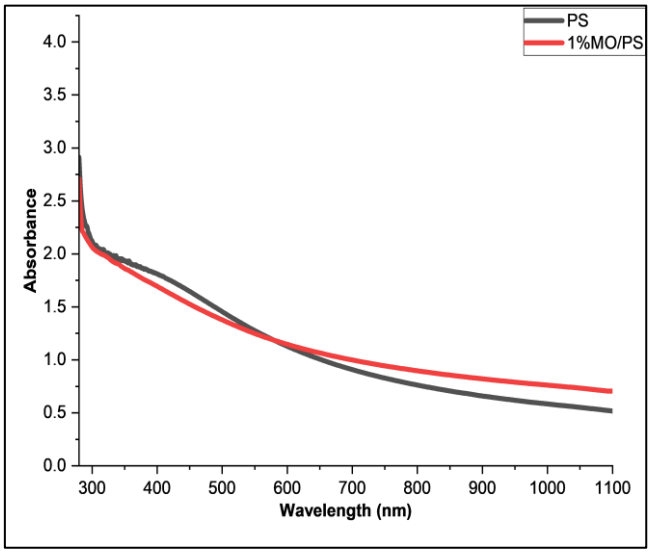

Figure 3. Comparison of absorption spectra for neat PS and MO/PS films before gamma irradiation.

3.2 Absorption Spectra of PS & MO/PS Before Gamma Irradiation

Figures (3&4) showed the optical absorption spectra of irradiated films for PS and MO/PS before and after irradiation. The absorption spectra for all films were obtained within a range of 280–1100 nm at three doses (1.0 kGy, 5.0 kGy and 10 kGy). The $\pi \rightarrow \pi^*$ electronic transition was responsible for the maximum absorbance peak that was located at 280 nm for all the films. Irradiation's primary effects include chain scission, cross-linking, as well as the creation of unsaturated products in the polymer chain. Irradiation causes the polymer to produce free radicals, which can then react with atmospheric oxygen to form hydroxyl and carbonyl groups. The presence of carbonyl and hydroxyl groups in PS, and the creation of unsaturated groups was probably the main reason associated with the increment of absorbance upon gamma irradiation [15, 33, and 34]. The absorption decreased monotonically into the visible range after reaching its maximum value at 280 nm. Carbonium ion formation, which may be resulted from the interaction of ray-induced free radicals with conjugated structure, was responsible for the long tail in the visible region [15, 35]. It was evident that the absorption was moving towards the longer wavelengths, and gradually increased with absorbed doses.

This behavior can be attributed to the chemical reaction generated by ionizing radiation in polymers, which affected both the molecular structure and macroscopic characteristics. As a result, degradation products represented by electrons and holes were created in parallel with samples' exposure to radiation, which consequently altered the optical absorbance [25]. The systematic promotion of the optical features with the absorbed doses of radiation inspires the optimism about the possibility of utilizing the prepared samples in sophisticated applications represented by dosimeters.

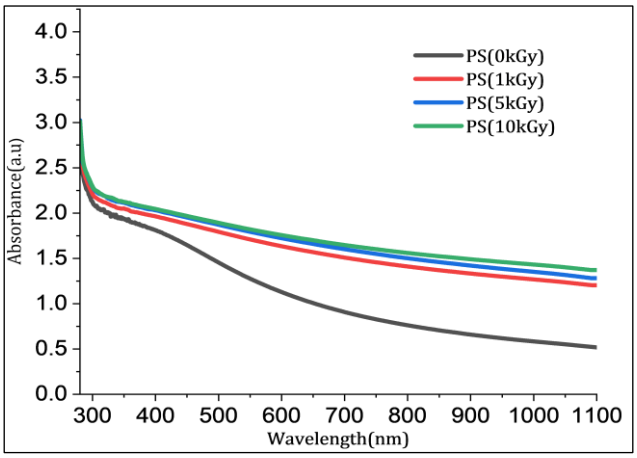

Figure 4. The absorption spectra for neat PS before and after exposure of gamma ray.

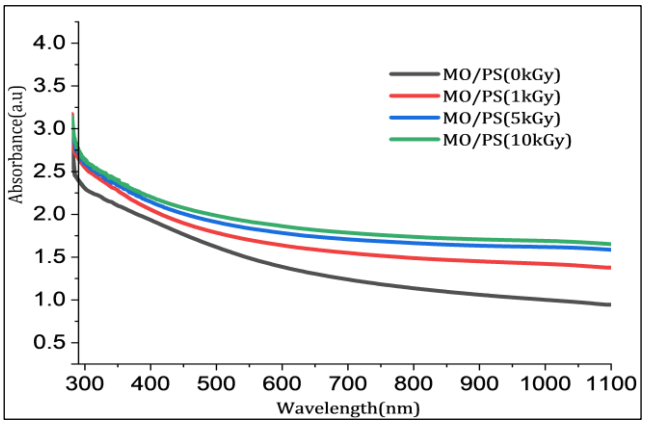

Figure 5. The absorption spectra for MO/ PS before and after exposure of gamma ray

3.3 Energy Gap of PS & MO/PS Before Gamma Irradiation

Band gaps, both direct and indirect Tauc's model is utilized to estimate Eg as follows: [36-39]

$$[(\alpha h\upsilon)]^m = A\,(h\upsilon - E_g) \quad (1)$$

The direct transition band gap was described at m = 2.0, and the indirect allowed transition was assumed to occur at m = 1/2, where A is an independent constant related to photon energy(hυ). where is, h is Planck's constant is the frequency of light. The symbol α is the absorption coefficient and Eg is the optical band gap energy. A photon cannot be released in an indirect gap since the electron needs to transfer momentum to the crystal lattice, and go through an intermediate state. Figures 6 and 7 showed the data of $(\alpha h\upsilon)^{1}/^{2}$ with the variation of the photon energy (hυ) for MO/PS films and pure PS films. The linear portions were fitted to the x-axis at $(\alpha h\nu)^{1}/^{2} = 0$ to obtain the band gaps. The direct band gap transition and the evolution of the polymeric films' band gaps were nearly identical. It was noticed that the energy gap for PS was (4.25 eV) before irradiation, and then decreased to be (4.13 eV) after adding methyl orange dye. This outcome was due to the increase in local potentials within the energy gap, which is agree with previously reported studies [31, 40, and 41]. All band gaps energies decreased with further doses of gamma rays. The energy gap was decreased linearly with the exposure to the irradiation dose, which was explained by an increase in interface traps, and localized states with the irradiation dose. [33,42].

An increase in the structural disorder of the irradiated dyed PS may played a special role in the decrement of the band gap energy in parallel with increasing the radiation dose. The systematic decrement in energy gap for all samples with absorbed dose support the research orientation of using the prepared samples as a dosimeter within this range as regarded in previous sections. These samples contributed to

achieve the structural defects, which has a role in increasing the width of the localized states, and consequently reducing the value of the optical gap [1,37,43, and 44].

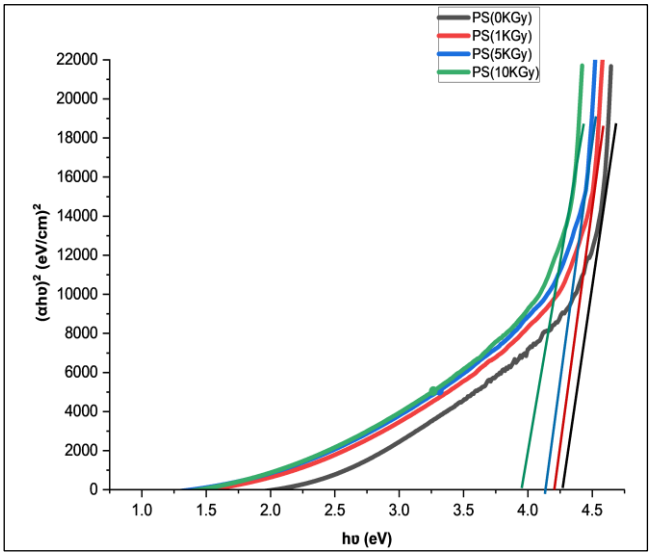

Figure 6. (αhυ)2 against (hυ) for PS before and after gamma radiation at (1,5 & 10 KGy) doses.

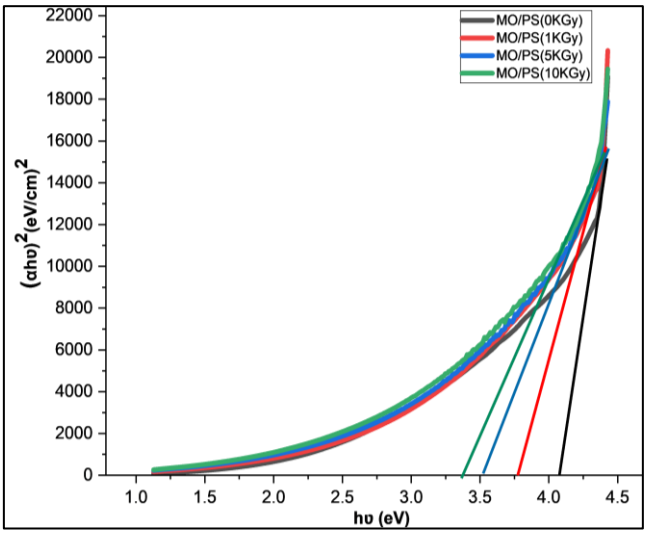

Figure 7. (αhυ)2 against (hυ) for MO/PS before and after gamma radiation at (1,5 & 10 KGy) doses.

3.4 Absorption Coefficient of PS & MO/PS Before Gamma Irradiation

By using Lambert's law as a guide, the absorption coefficient (α) of the absorption edge was found [45-48]:

$$\alpha = \frac{2.303 \times A}{t} \qquad (2)$$

Where t is the sample thickness, and A is the measured absorbance. Figures (8&9) shows the absorption coefficient of the PS and the other MO/PS composites before and after radiation with a dose of γ-rays, which was varied between (1.0 - 10 kGy). The figures showed that the absorption coefficient increased with the irradiation dose. This was ascribed to changes in absorption brought by photo-degradation, which was brought by radiation's increase in localized state [33, 49].

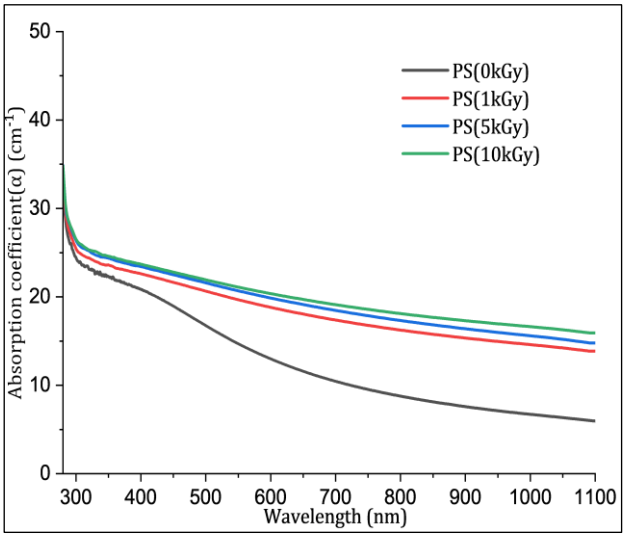

Figure 8. The relationship between PS's wavelength and absorption coefficient before and after three doses of gamma radiation.

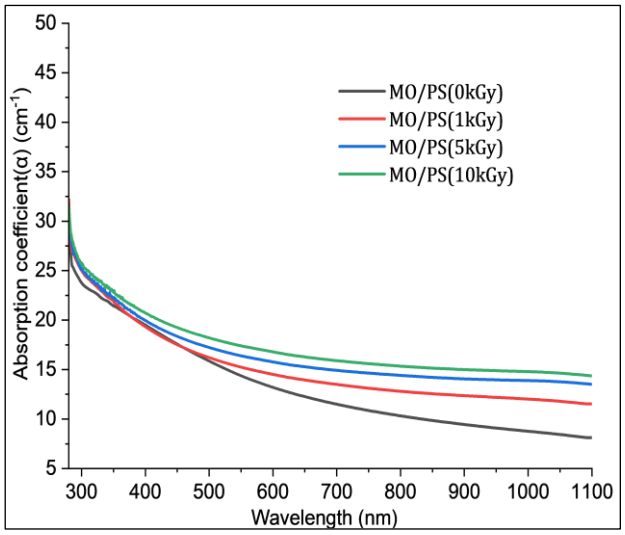

Figure 9. The relationship between MO/PS's wavelength and absorption coefficient before and after three doses of gamma radiation.

3.5 Extinction Coefficient of PS & MO/PS Before Gamma Irradiation

The extinction coefficient (K) could be obtained from the following equation [50-52]:

$$K = \frac{\lambda\alpha}{4\pi} \quad (3)$$

λ is the wavelength.

Figures (10 &11) give an interpretation about the coefficient (K) behavior, which was almost identical to that one of the corresponding absorption coefficients(α)shown in figures (8 &9). This outcome is in a good agreement with what was previously reported[1,25]. For the abovementioned reasons, the increment in absorption coefficient urged the extinction coefficient to rise with the irradiation dose; its peaks shifted toward long wavelengths, which was ascribed to a narrowing of the energy gap with the irradiation dose.

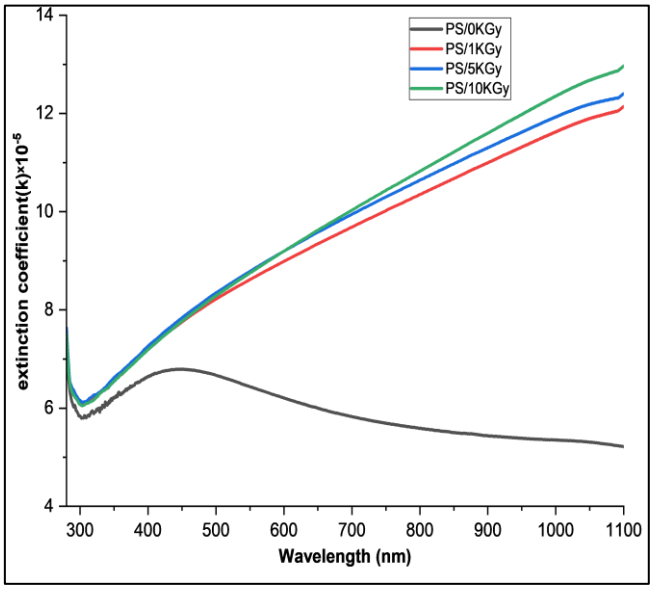

Figure 10. Relation between the extinction coefficient and wavelength of PS before and after gamma radiation for three doses.

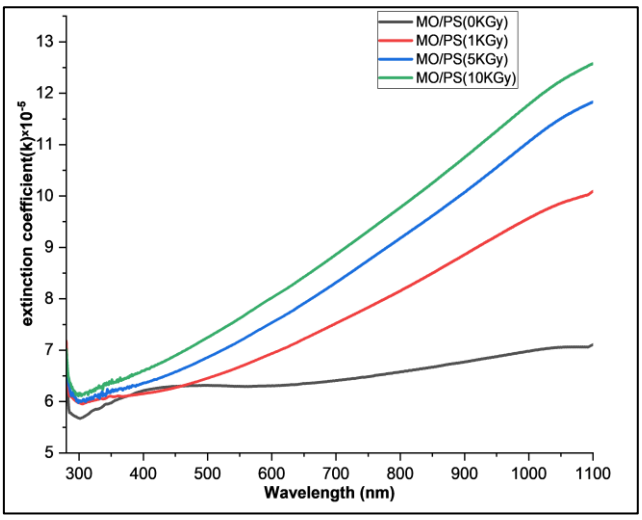

Figure 11. Relation between the extinction coefficient and wavelength of MO/PS before and after gamma radiation for three doses.

3.6 FTIR Spectra of PS and MO/PS Samples Before and After Gamma Irradiation

With gamma irradiation, FTIR was used to determine the molecular structures of both PS as well as the irradiated and non-irradiated MO/PS composites. The spectrum of the virgin PS and MO/PS films before irradiation is shown in Figure 12 and table 1. It was noted that three bands appeared at the range (2800-3060cm^{-1}), which was ascribed to the C-H stretching of the aromatic and aliphatic groups; respectively. As shown in previous studies [53,54], the peak located at 3445.51cm^{-1} was related to O-H stretching, and the peaks located at (1315.45 and 1338.60 cm^{-1}) was attributed to the symmetrical and asymmetrical stretching vibration of CH2 bands. The peak located at 1598.99 cm^{-1} was related to stretching vibration of the C=C bond on the benzene ring, whereas bands at 908.47 and 941.26 cm-1 are attributed to C-O bond. Five bands varied from (630 – 908 cm-^{1})are linked to the C-H out-of-plane bending vibration of the benzene ring [55, 56]. On the other hand, the spectra of (MO/PS) films exhibited similar behavior compared to pure PS. The band appeared at1600 cm-1 confirmed the presence of wagging C=C and the small shift occurred at 3564.64 cm^{-1} assigned to the stretching of O-H groups on films surfaces. It was noticed that the band of C-H beyond the plane bending was also related to the five bands. There was a shifting in almost bands, which was connected to the benzene ring hydrogen's C-H deformation vibration band. The C-O stretch appeared at (906.54 and 943.19 cm^{-1}) were vanished at C-H aliphatic, and at C-H aromatic; respectively. There was a physical interaction between the PS and MO ascribed to the variation into the band location (shifting) of the PS aromatic ring, which is in line with the literature [57, 58].

The powder of MO's spectra, which was exhibited at a range of 600–4000 cm^{-1}, included the typical bands of the azo band (-NΞN-) at (1317–600 cm^{-1}), and the benzene ring, which was obvious at (1400–1602 cm^{-1}). The symmetric and antisymmetric stretching vibration at (-CH_2) appeared at (2820–2903 cm^{-1}). In addition, the asymmetrical stretching vibration of (-SO_3Na) set was attributed to the typical band at 1004 cm^{-1}. This outcome is in a good

agreement with the literature [45, 59]. After all films were exposed to gamma radiation at doses of 1, 5, and 10 kGy, FTIR spectra were obtained for each sample.it is noticed that FTIR spectra lightly change especially after irradiation with doses (5.0 and 10 kGy) for all (pure PS and MO/PS) as shown in table (1) as well as Figures (13 and 14).

Compared to non-irradiated PS, irradiated PS bands were influenced by radiation. They became broader and less intense, indicating structural changes brought by gamma irradiation. This outcome is in line with a previously reported study [14, 60]. It is emphasized that intensity of the band at 1591.27 cm^{-1} that corresponds to C=C stretching decreased as a result of gamma radiation, and disappeared at 630.72 cm-1 at doses of (5.0 and 10 kGy) for C-H out of phase pending. Moreover, bands at 964.41 cm^{-1} of C-O stretching were appeared at the dose of 1.0 kGy, and disappeared again at the doses of (5.0 and 10 kGy). With high dose of 10kGy, there was a disappearance of band 2835.36 cm-1 from the aromatic bond, and shifting towards longer wavelengths from 3445.51 to 3566.38 cm^{-1} O-H hydroxyl stretching.

However, in MO/PS, the spectrum changed clearly, and it was evident that MO dye made an impact on it. The C-H band denoted the ring deformation vibration in the region of (625-910) cm^{-1}. MO dye, which refers to (C-H) bending vibration and gamma effect, caused the reappearance of the peak of (667.37) cm^{-1} at 10 kGy after its disappearance at doses of 1.0 and 5.0 kGy due to the (C-H) deformation vibration band of benzene ring hydrogens. Furthermore, the benzene ring was specifically referenced by the peak at (1598.99) cm^{-1} for (C=C) stretching at dose of 10 kGy, which was related to MO dye, and gamma effect as well [61, 62]. At a range of (1300-1380 cm^{-1}) due to CH2 bending, there was shifting at band (1336.67 cm^{-1}). A new band appeared at doses of (1.0 and 5.0 kGy), and disappeared at the dose of 10 kGy. In addition, a new band appeared at 1327.03 cm^{-1}. At all doses, new bands appeared for C-H stretching aliphatic and aromatic [63, 64].

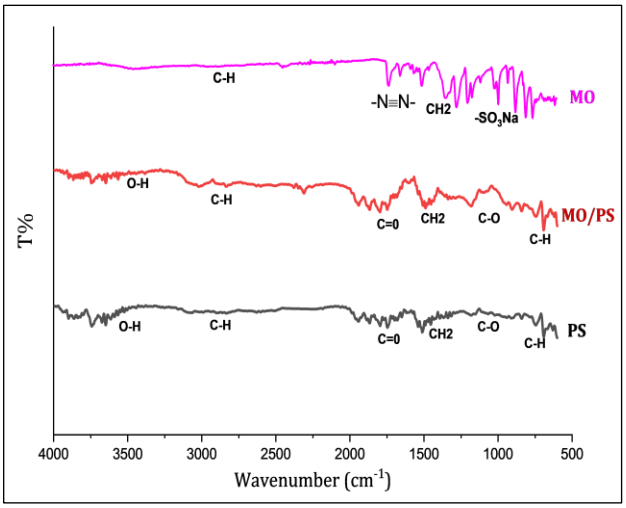

Figure12. FTIR Spectra of PS before and after doping with methylene orange(MO.)

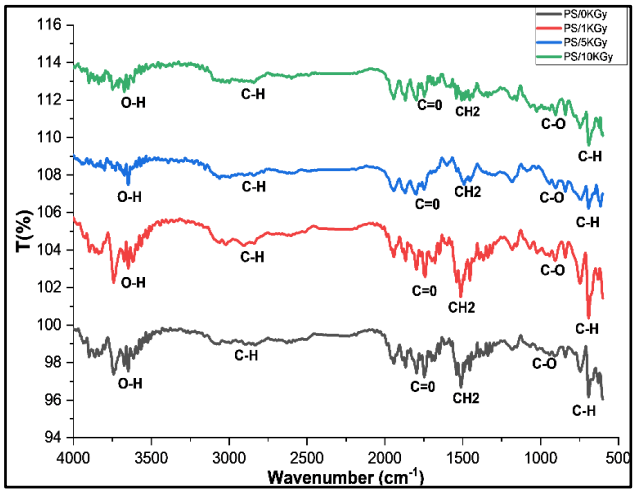

Figure (13): FTIR Spectra of PS before and after gamma ray exposure at three doses.

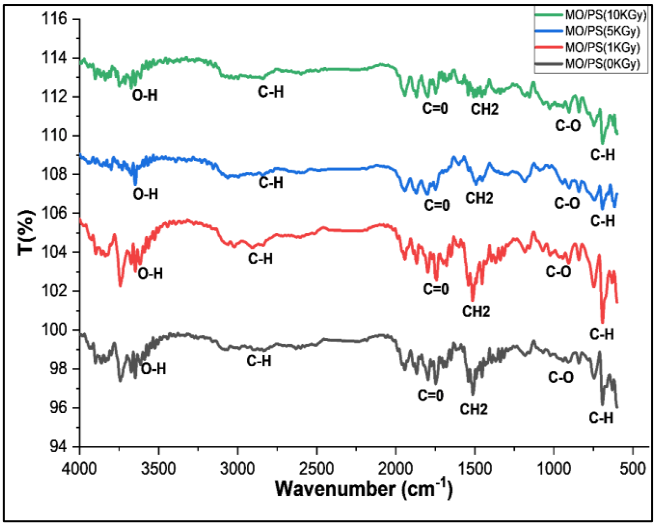

Figure (14): FTIR Spectra of MO/PS before and after gamma ray exposure at three doses.

3.7 Morphology

PS and MO/PS membranes must undergo morphological analysis in order to assess the material's surface features and structural properties before and after exposure ɣ-ray. Figure 15 showed the optical micrographs of pure PS films captured at doses of 1.0, 5.0, and 10 kGy before and after gamma irradiation. As shown in (a), PS was free of defects and bubbles prior to irradiation, indicating that no evidence of porous structure in the sample. The most notable effect of 1.0 kGy radiation was the release of gas. For the micrographs of (b-c), bubbles may form, and as dosage increased, more holes and grooves may become visible. Similar observations were previously reported[63, 64]. As observed in dose (10 kGy), PS photodegraded in the presence of oxygen, leading to deterioration and crack formation. When degradation occurred, the bubbles were burst as shown in micrograph (d), which is in line with the literature [65, 66]. While singlet oxygen undergoes a number of distinct reactions, the most common one in the photo-oxidation of polymers was the creation of a hydro-peroxide through the oxidation of an olefin that contained an allylic hydrogen. This can then further break down, resulted in chain scission, and led to the formation of a carbonyl group terminal[65, 67].

Figure (16) shows that MO/PS was homogenous, and it had a bubble-free morphology with a few clusters of methyl orange as shown in micrograph (a), but no indication of a porous structure in the sample. The most notable result of high doses of radiation as shown in micrographs of (b–c) was the release of gas. As radiation dosages increased, more bubbles, rough surfaces, and lines (holes or grooves) were revealed. Similar morphological findings were reported [63, 68]. The majority of the bubbles burst at high dose irradiation (10 kGy) as shown in micrograph (d), whereas oxygen caused structural deterioration and crack formation. These cracks were increased, and clustering decreased with absorbed doses[65, 69].

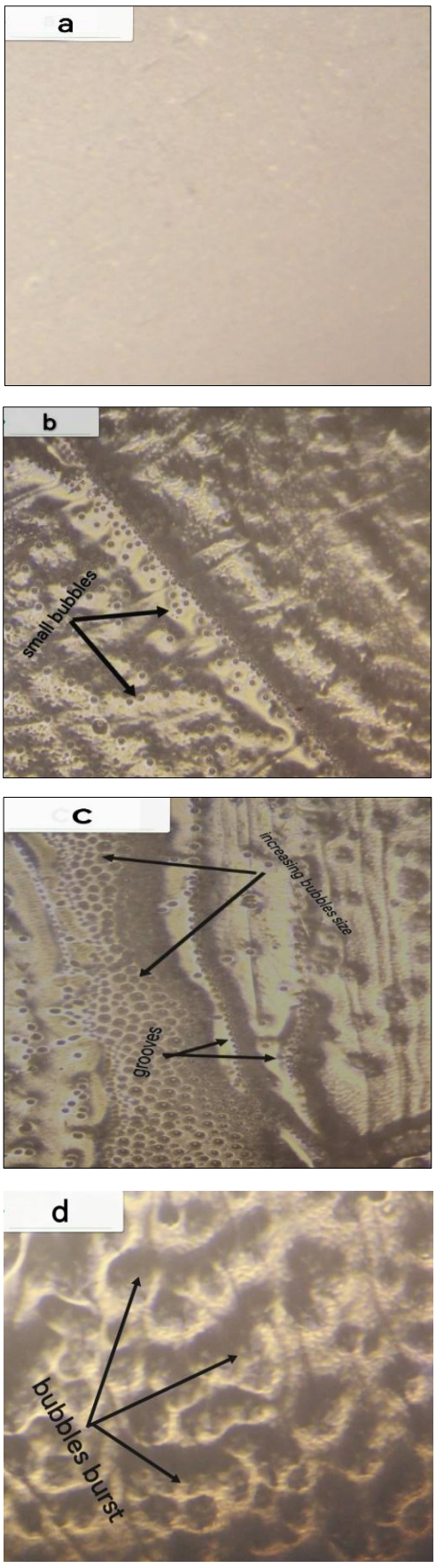

Figure 15. Optical micrographs of (a) pure PS film before gamma irradiation, and after irradiation with 1kGy (b), 5kGy (c), 10kGy(d).

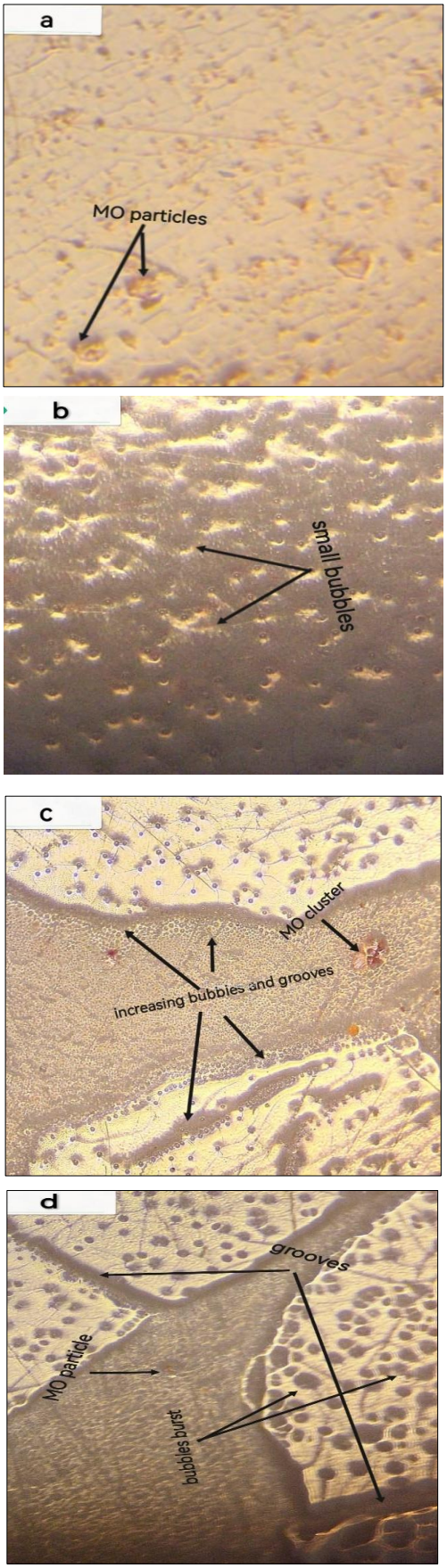

Figure 16. Optical micrographs of (a)MO/PS film before gamma irradiation, and after irradiation with 1kGy (b), 5kGy (c), 10kGy(d).

Table 1 FTIR-characteristic of PS and MO/PS before and after gamma ray exposure to three doses

Polymer System	(C-H) out of phase bending 625-910 cm^{-1}	(C-O) Stretching 880-1010 cm^{-1}	(CH2 -) Bending 1300-1380 cm^{-1}	(CH2) Wagging C=C Stretching 1550-1610 cm^{-1}	(C=O) Stretching 1550-1750 cm^{-1}	(C-H) Stretching Elphatic 2800-3000 cm^{-1}	(C-H) Stretching Aromatic 2800-3060 cm^{-1}	(O-H) Hydroxyl Stretching 3340-3600 cm^{-1}
PS (0kGy)	630.72 692.44 744.52 840.96 908.47	908..47 941.26	1315.45 1338.60	1598.99	1618.28 1651.07 1681.93 1747.51	2835.36 2889.37 2991.59	2835.36 2889.37 2991.59	3445.51
PS (1kGy)	632.65 690.52 746.45 840.96 906.54	906.54 943.19 964.41	1315.45 1338.60 1367.53	1598.99	1598.99 1651.07 1678.07 1741.72	2839.22 2904.80	3020..53 2839.22 2904.80 3020.53	3445.51
PS (5kGy)	692.44 740.67 840.96 902.69	902.69 943.19	1336.67	1600.92	1600.92 1678.07 1749.44	2833.43 2902.87 2993.52	2833.43 2902.87 2993.52	3560.86
PS (10 kGy)	690.52 746.45 840.96 902.69	902.69 941.26	1338.60	1591.27	1591.27 1651.07 1681.93 1747.51	2841.15 2999.31	2999.31 3101.54	3566.38
MO/PS (0kGy)	667.37 692.44 744.52 840.96 906.54	906.54 943.19	1315.45 1336.67	1600.92	1600.92 1651.07 1681.93 1747.51	2835.36	2835.36 3014.74	3564.43
MO/PS (1kGy)	690.52 742.59 840.96 906.54	906.54 943.19 966.34	1315.45 1338.60 1365.60	1600.92	1600.92 1678.07 1747.51	2858.51 2939.52	2858.51 2939.52 3072.60	3525.88
MO/PS (5kGy)	962.44 744.52 840.96 906.54	906.54 962.48	1315.45 1338.60 1367.53	1600.92	1600.92 1651.07 1681.93 1747.51	2858.51 2933.73	2858.51 2933.73	3523.95
MO/PS (10 kGy)	630.72 694.37 748.38 840.96 906.6	904.61 941.26	1327.03	1598.99	1598.99 1749.44	2843.07 2918.30	2843.07 2918.30 3022.45	3520.09

4. CONCLUSION

According to UV-vis spectroscopic studies of pure PS, and dyed unirradiated and irradiated films The highest absorbance appeared at 280 nm, and it rapidly decreased at wavelengths above 300 nm. Irradiation led to form free radicals in the polymer, and these radicals can react with oxygen in the air to compose carbonyl and hydroxyl groups. The absorption mechanism was identified as a direct allowed transition based on the optical absorption spectra, and the optical band gap. The decreased energy band gaps with the increased dose can be attributed to the increasing localized state, and interface traps that were induced by irradiation of the polymer film as the dose increased. The systematic decreasing in energy gap for both films with absorbed dose suggested the possibility of their employment as efficient dosimeters within the range of (1.0, 5.0 and 10 kGy).

Both of absorption and extinction coefficient increased with increasing radiation dose for PS and MO/PS composites. The formation of a broad vibrational peak around 3445.51 cm^{-1} for PS film, and around 3564.43 cm^{-1} for MO/ PS film was emphasized by FTIR findings. This is because the -OH group absorbed moisture before and after irradiation by the ɣ-ray. The PS and MO interacted physically, which was explained by the PS aromatic ring's shifting or changing band location, and these interactions were increased after applying gamma radiation.

ACKNOWLEDGEMENTS

This work was supported by physics department at science collage in Baghdad university and Bpc Analysis Center.

REFERENCE

[1] T. J. Alwan, «Gamma irradiation effect on the optical properties and refractive index dispersion of dye doped polystyrene films», Turkish J. Phys., vol. 36, n. 3, pagg. 377–384, 2012, doi: 10.3906/fiz-1107-5.

[2] Abdul Muhsien M.; Salem E. T.; Agool I.R., Preparation and characterization of (Au/n-Sn O2 /Si O2 /Si/Al) MIS device for optoelectronic application, International Journal of Optics, 2013, 756402 (2013) 10.1155/2013/756402.

[3] Khawla S. Khashan, Aseel A. Hadi, Rana O. Mahdi & Doaa S. Jubair, Aluminum-doped zinc oxide nanoparticles prepared via nanosecond Nd: YAG laser ablation in water: optoelectronic properties, Opt Quant Electron 56, 125 (2024). https://doi.org/10.1007/s11082-023-05630-x.

[4] Jurn Y. N.; Malek F.; Mahmood S. A.; Liu W.-W.; Fakhri M. A.; Salih M. H., Modelling and simulation of rectangular bundle of single-walled carbon nanotubes for antenna applications Key Engineering Materials, 701, 57-66 (2016) 10.4028/www.scientific.net/KEM.701.57.

[5] M. F. H. Al-Kadhemy, A. A. Saeed, R. I. Khaleel, e F. J. K. Al-Nuaimi, «Effect of gamma ray on optical characteristics of (PMMA/PS) polymer blends», J. Theor. Appl. Phys., vol. 11, n. 3, pagg. 201–207, 2017, doi: 10.1007/s40094-017-0259-7.

[6] Fakhri M. A.; Al-Douri Y.; Hashim U., Fabricated Optical Strip Waveguide of Nanophotonics lthium Niobate, IEEE Photonics Journal, 8(2), 7409919 (2016) 10.1109/JPHOT.2016.2531583.

[7] T. Swu, C. A. Pongener, D. Sinha, e N. L. Sen Sarma, «Effect of gamma radiation on dielectric properties of polyacetate polymer», Pelagia Res. Lib, vol. 4, n. 3, pagg. 132–136, 2013.

[8] Zainab T. Hussain, Khawla S. Khashan, Rana O. Mahdi, Characterization of cadmium oxide nanoparticles prepared through Nd:YAG laser ablation process, Materials Today: ProceedingsVolume 42, Pages 2645 – 26482021. https://doi.org/10.1016/j.matpr.2020.12.594.

[9] S. Baccaro, V. Brunella, A. Cecilia, e L. Costa, «$γ$ irradiation of poly (vinyl chloride) for medical applications», Nucl. Instruments Methods Phys. Res. Sect. B Beam Interact. with Mater. Atoms, vol. 208, pagg. 195–198, 2003.

[10] Roaa A. Abbas, Evan T. Salim & Rana O. Mahdi, Deposition time effect on copper oxide nano structures, an analysis study using chemical method, J Mater Sci: Mater Electron 35, 427 (2024). https://doi.org/10.1007/s10854-024-12143-0.

[11] A. Abdullah, «The effect of high irradiation energy (Gamma, UV-light) Radiation on the energy gap of polymers doped with Anthrancene», Iraqi J. Sci., vol. 47, n. 1, pagg. 99–103, 2006.

[12] B. Alshahrani, «Effect of Gamma Irradiation on the Structural , Optical , and Electronic Properties of PVC / BiVO 4 / ZnO Nanocomposite Films», pagg. 1–25, 2024.

[13] H. H. Mohammed, Z. N. Majeed, e Z. K. Abbas, «Investigation of optical properties of irradiated and unirradiated poly (vinyl chloride-co-vinyl acetate)», vol. 10, n. 1, pagg. 134–141, 2012.

[14] J. A. Yabagi, M. I. Kimpa, M. N. Muhammad, S. Bin Rashid, E. Zaidi, e M. A. Agam, «The effect of gamma irradiation on chemical, morphology and optical properties of polystyrene nanosphere at various exposure time», IOP Conf. Ser. Mater. Sci. Eng., vol. 298, n. 1, 2018, doi: 10.1088/1757-899X/298/1/012004.

[15] Lobo, Blaise others «Optical properties and structural features of UV-C irradiated polyvinylidene chloride lms Abstract »:, 2022.

[16] N. J. Hameed, A. J. Haider, e R. E. Hawy, «Optical properties study for PS/PMMA blend as laser active medium», in AIP Conference Proceedings, 2019.

[17] Fakhri M. A.; Wahid M. H. A.; Kadhim S. M.; Badr B. A.; Salim E. T.; Hashim U.; Salim Z.T., The structure and optical properties of Lithium Niobate grown on quartz for photonics application, EPJ Web of Conferences, 162, 1005 (2017) 10.1051/epjconf/201716201005

[18] H. A. Hadi, R. A. Ismail, e N. J. Almashhadani, «Preparation and characteristics study of polystyrene/porous silicon photodetector prepared by electrochemical etching», J. Inorg. Organomet. Polym. Mater., vol. 29, n. 4, pagg. 1100–1110, 2019.

[19] X. Xu, R. W. M. Kwok, e W. M. Lau, «Surface modification of polystyrene by low energy hydrogen ion beam», Thin Solid Films, vol. 514, n. 1–2, pagg. 182–187, 2006, doi: 10.1016/j.tsf.2006.02.095.

[20] H. Abed, N. Hameed, e E. Salim, «Study of Mechanical and Optical Properties of Nano-hydroxyapatite Dispersed PS/PC Blend Nanocomposites», Int. J. Nanoelectron. Mater., vol. 17, n. 1, pagg. 122–127, 2024, doi: 10.58915/ijneam.v17i1.496.

[21] R. A. Ismail, N. J. Almashhadani, e R. H. Sadik, «Preparation and properties of polystyrene incorporated with gold and silver nanoparticles for optoelectronic applications», Appl. Nanosci., vol. 7, pagg. 109–116, 2017.

[22] H. Abed, N. J. Hameed, e E. T. Salim, «Influence of nano-hydroxyapatite particles on the mechanical and antibacterial properties of polycarbonate films», Mater. Res. Express, vol. 10, n. 8, 2023, doi: 10.1088/2053-1591/acec35.

[23] S. Bhavsar, N. L. Singh, e K. V. R. Murthy, «Comparative Study of Impact of Gamma and MeV Ion Irradiations on Electrical and Optical Properties Polystyrene/Eu2O3 Nanocomposites», J. Fluoresc., n. 0123456789, 2023, doi: 10.1007/s10895-023-03425-7.

[24] V. R. Sastri, «Commodity Thermoplastics: Polyvinyl Chloride, Polyolefins, Cycloolefins and Polystyrene», Plast. Med. Devices, vol. 113, pagg. 113–166, 2022, doi: 10.1016/b978-0-323-85126-8.00002-3.

[25] M. Demirors, «Styrene polymers and copolymers», Appl. Polym. Sci. 21st Century, vol. 1, 2000.

[26] D. J. Thomas, «3D printing techniques in medicine and surgery», in 3D Printing in Medicine and Surgery, Elsevier, 2021, pagg. 15–45.

[27] G. J. Habi, «Study the optical characteristics of polystyrene polymer before and after doping with methyl orange», Period. Eng. Nat. Sci., vol. 9, n. 4, pagg. 368–374, 2021, doi: 10.21533/pen.v9i4.2333.

[28] M. F. Barakat e M. El-Banna, «Use of some organic dyes in gamma irradiation dose determination», J. Radioanal. Nucl. Chem., vol. 287, n. 2, pagg. 367–375, 2011, doi: 10.1007/s10967-010-0894-9.

[29] Evan T. Salim, Ahmed T. Hassan, Rana O Mahdi, Forat H. Alsultany, Physical Properties of HfO2 Nano Structures Deposited using PLD, IJNeaM, vol. 16, no. 3, pp. 495–510, Oct. 2023.

[30] A. Marzec, «The effect of dyes, pigments and ionic liquids on the properties of elastomer composites», Université Claude Bernard-Lyon I; Uniwersytet łódzki, 2014.

[31] N. J. H. Al-Mashhadan e S. Mohamad, «Study of degradation effect on physical properties of methyl orange doped PMMA», J. Eng. Technol, vol. 29, n. 1, pagg. 20–32, 2011.

[32] T. J. Alwan, «Refractive index dispersion and optical properties of dye doped polystyrene films», Malaysian Polym. J., vol. 5, n. 2, pagg. 204–213, 2010.

[33] N. J. H Al-Mashhada, «γ-Irradiation Effect on the Optical Constants, and the Electric Loss of PM-355», Eng. Technol. J., vol. 32, n. 6B, pagg. 1158–1168, 2014, doi: 10.30684/etj.32.6b.15.

[34] Jurn Y. N.; Malek F.; Mahmood S. A.; Liu W.-W.; Gbashi E. K.; Fakhri M. A., Important parameters analysis of the single-walled carbon nanotubes composite materials, ARPN Journal of Engineering and Applied Sciences, 11(8), 5108-5113 (2016).

[35] Rana O. Mahdi, Aseel A. Hadi, Juhaina M. Taha, Khawla S. Khashan, Preparation of nickel oxide nanoparticles prepared by laser ablation in water, AIP Conf. Proc. 2213, 020309 (2020) https://doi.org/10.1063/5.0000116.

[36] G. Geetha, M. Priya, e S. Sagadevan, «Investigation of the optical and electrical properties of tin sulfide thin films», Chalcogenide Lett., vol. 12, n. 11, pagg. 609–617, 2015.

[37] A. Arshak, S. Zleetni, e K. Arshak, «γ-Radiation sensor using optical and electrical properties of manganese phthalocyanine (MnPc) thick film», Sensors, vol. 2, n. 5, pagg. 174–184, 2002, doi: 10.3390/s20500174.

[38] Khawla S khashan, Rana O Mahdi, Ban A. Badr, Farah Mahdi, Preparation and characterization of ZnMgO nanostructured materials as a photodetector, Journal of Physics: Conference Series 1795 (2021) 012008. doi:10.1088/1742-6596/1795/1/012008.

[39] Aseel A. Hadi, Juhaina M. Taha, Rana O. Mahdi, Khawla S. Khashan, Influence of laser pulse on properties of NiO NPs prepared by laser ablation in liquid, AIP Conf. Proc. 2213, 020308 (2020) https://doi.org/10.1063/5.0000115.

[40] K. M. Ali e N. J. H, «Study of Methyl Orange Effect on the Optical and Electrical Properties of Polystyrene (PS)», Eng. Technol. J., vol. 32, n. 6B, pagg. 39–53, 2014, doi: 10.30684/etj.32.6b.17.

[41] S. A. Nouh, S. J. Alsufyani, N. Gweily, C. V. More, e M. M. E. Barakat, «Gamma Ray Irradiation Induced Changes in Polycarbonate/Zinc Sulfide-Cerium Oxide Nanocomposite Films. Optical and Color Modifications», J. Macromol. Sci. Part B Phys., n. February, 2025, doi: 10.1080/00222348.2025.2461397.

[42] Azzam Y. kudhur, Evan T. Salim, Ilker Kara, Rana O. Mahdi & Raed K. Ibrahim, The effect of laser energy on Cu2O nanoparticles formation by liquid-phase pulsed laser ablation, J Opt 53, 1309–1321 (2024). https://doi.org/10.1007/s12596-023-01319-2

[43] E. A. Kamoun et al., «Effect of gamma irradiation on the electrical and optical properties of PEVA composite membrane embedded with conductive copper fluoroborate glass powder», Mater. Adv., vol. 5, n. 13, pagg. 5658–5670, 2024, doi: 10.1039/d4ma00328d.

[44] Hassen H. H.; Salim E. T.; Taha J. M.; Mahdi R. O.; Numan N. H.; Khalid F. G.; Fakhri M. A., Fourier transform infrared spectroscopy and photo luminance results for Zno NPs prepared at different preparation condition using LP-PLA technique, International Journal of Nanoelectronics and Materialsm, 11(Special Issue BOND21) 65-72 (2018).

[45] W. Jilani, A. Bouzidi, I. S. Yahia, H. Guermazi, H. Y. Zahran, e G. Saker, «Effect of organic dyes on structural properties, linear optics and impedance spectroscopy of methyl orange (C.I. acid orange 52) doped polyvinyl alcohol composite thin films», J. Mater. Sci. Mater. Electron., vol. 29, n. 19, pagg. 16446–16453, 2018, doi: 10.1007/s10854-018-9736-2.

[46] F. Yakuphanoglu, M. Sekerci, e E. Evin, «The determination of the conduction mechanism and optical band gap of fluorescein sodium salt», Phys. B Condens. Matter, vol. 382, n. 1, pagg. 21–25, 2006, doi: https://doi.org/10.1016/j.physb.2006.01.511.

[47] Fakhri M. A.; Al-Douri Y.; Bouhemadou A.; Ameri M., Structural and Optical Properties of Nanophotonic LiNbO3 under Stirrer Time Effect, Journal of Optical Communications, 39(3), 297-306 (2018) 10.1515/joc-2016-0159.

[48] Roaa A. Abbas, Evan T. Salim & Rana O. Mahdi, Morphology transformation of Cu2O thin film: different environmental temperatures employing chemical method, J Mater Sci: Mater Electron 35, 1057 (2024). https://doi.org/10.1007/s10854-024-12823-x.

[49] Fakhri M. A.; Numan N. H.; Mohammed Q. Q.; Abdulla M. S.; Hassan O. S.; Abduljabar S. A.; Ahmed A. A., Responsivity and response time of nano silver oxide on silicon heterojunction detector, International Journal of Nanoelectronics and Materials, 11(Special Issue BOND21), 109-114 (2018)

[50] Fakhri M. A.; Wahid M. H. A.; Badr B. A.; Kadhim S. M.; Salim E. T.; Hashim U.; Salim Z.T., Enhancement of Lithium Niobate nanophotonic structures via spin-coating technique for optical waveguides application, EPJ Web of Conferences, 162, 1004 (2017) 10.1051/epjconf/201716201004.

[51] Azzam Y. Kudhur, Evan T. Salim, Ilker Kara, Makram A. Fakhri & Rana O. Mahdi, Structural optical and morphological properties of copper oxide nanoparticles ablated using pulsed laser ablation in liquid, J Opt 53, 1936–1945 (2024). https://doi.org/10.1007/s12596-023-01331-6.

[52] Muhsien M. A.; Salem E. T.; Agool I. R.; Hamdan H. H., Gas sensing of Au/n-SnO2/p-PSi/c-Si heterojunction devices prepared by rapid thermal oxidation, Applied Nanoscience (Switzerland), 4(6), 719-732 (2014) 10.1007/s13204-013-0244-7.

[53] H.-D. Wu, S.-C. Wu, I.-D. Wu, e F.-C. Chang, «Novel determination of the crystallinity of syndiotactic polystyrene using FTIR spectrum», Polymer (Guildf)., vol. 42, n. 10, pagg. 4719–4725, 2001.

[54] P. V. Vardhan e L. I. Shukla, «Ft-ir investigations on effect of high doses of gamma radiationinduced damage to polystyrene and mechanism of formation of radiolysis products», Radiat. Environ. Biophys., vol. 57, n. 3, pagg. 301–310, 2018, doi: 10.1007/s00411-018-0740-y.

[55] H. M. Eyssa, M. Osman, S. A. Kandil, e M. M. Abdelrahman, «Effect of ion and electron beam irradiation on surface morphology and optical properties of PVA», Nucl. Sci. Tech., vol. 26, n. 6, 2015.

[56] H. Yoon, J. Lee, D. W. Park, C. K. Hong, e S. E. Shim, «Preparation and electrorheological characteristic of CdS/Polystyrene composite particles», Colloid Polym. Sci., vol. 288, pagg. 613–619, 2010.

[57] Mohammed D. A.; Kadhim A.; Fakhri M. A., The enhancement of the corrosion protection of 304 stainless steel using Al2O3 films by PLD method, AIP Conference Proceedings, 2045, 20014 (2018) 10.1063/1.5080827.

[58] E. S. Džunuzović, J. V Džunuzović, A. D. Marinković, M. T. Marinović-Cincović, K. B. Jeremić, e J. M. Nedeljković, «Influence of surface modified TiO2 nanoparticles by gallates on the properties of PMMA/TiO2 nanocomposites», Eur. Polym. J., vol. 48, n. 8, pagg. 1385–1393, 2012.

[59] Fakhri M. A.; Numan N. H.; Alshakhli Z. S.; Dawood M. A.; Abdulwahhab A. W.; Khalid F. G.; Hashim U.; Salim E. T., Physical investigations of nano and micro lithium-niobate deposited by spray pyrolysis technique, AIP Conference Proceedings, 2045, 20015 (2018) 10.1063/1.5080828.

[60] Tawfiq Z. H.; Fakhri M. A.; Adnan S. A., Photonic Crystal Fibres PCF for Different Sensors in Review, IOP Conference Series: Materials Science and Engineering, 454(1), 12173 (2018) 10.1088/1757-899X/454/1/012173

[61] M. F. H. Al-Kadhemy, M. Fadhel, H. Al-Kadhemy, W. H. Abaas, e I. Fakher, «The Effect of Gamma Radiation on the FTIR Spectrum of Crystal Violet Doped Polystyrene Films», Casp. J. Appl. Sci. Res., vol. 2, n. 7, pagg. 11–17, 2013.

[62] Doaa A. Mahmoud, Evan T. Salim, Rana O. Mahdi, A. Mindil, Subash C. B. Gopinath & Motahher A. Qaeed, Laser Ablation of Tungsten Metal for Au@WO3 Core-Shell Formation: A Characterizing Study at Different Laser Fluences, Plasmonics (2024). https://doi.org/10.1007/s11468-024-02607-8.

[63] J. A. Yabagi, M. I. Kimpa, M. N. Muhammad, S. Bin Rashid, E. Zaidi, e M. A. Agam, «The effect of gamma irradiation on chemical, morphology and optical properties of polystyrene nanosphere at various exposure time», in IOP Conference Series: Materials Science and Engineering, 2018, pag. 12004.

[64] Fakhri M. A.; Bader B. A.; Khalid F. G.; Numan N. H.; Abdulwahhab A. W.; Hashim U.; Salim E. T.; Munshid M. A.; Salim Z. T., Optical and morphological studies of LiNbO3 nano and micro photonic structural, AIP Conference Proceedings, 2045, 20017 (2018) 10.1063/1.5080830.

[65] E. Yousif e R. Haddad, «Photodegradation and photostabilization of polymers, especially polystyrene», Springerplus, vol. 2, pagg. 1–32, 2013.

[66] Jehan A. Saimon, Suzan N. Madhat, Khawla S. Khashan, Azhar I. Hassan, Rana O. Mahdi, Rafah A. Nasif, Synthesis of CdxZn1-xO nanostructure films using pulsed laser deposition technique, AIP Conf. Proc. 2045, 020003 (2018) https://doi.org/10.1063/1.5080816.

[67] Fakhri M. A.; Abdulwahhab A. W.; Dawood M. A.; Raheema A. Q.; Numan N. H.; Khalid F. G.; Wahid M. H. A.; Hashim U.; Salim E. T., Optical investigations of nano lithium niobate deposited by spray pyrolysis technique with injection of Li2CO3 and Nb2O5 as raw materials, International Journal of Nanoelectronics and Materials, 11(Special Issue BOND21), 103-108 (2018).

[68] Alsultany F. H.; Alhasan S. F. H.; Salim E. T., Seed Layer-Assisted Chemical Bath Deposition of Cu2O Nanoparticles on ITO-Coated Glass Substrates with Tunable Morphology, Crystallinity, and Optical Properties, Journal of Inorganic and Organometallic Polymers and Materials, 31(9), 3749-3759 (2021) 10.1007/s10904-021-02016-y.

[69] Fakhri M. A.; Salim E. T.; Wahid M. H. A.; Salim Z. T.; Hashim U., A novel parameter effects on optical properties of the LiNbO3 films using sol-gel method, AIP Conference Proceedings, 2213, 20242 (2020) 10.1063/5.0000206.